Progress In Electromagnetics Research, PIER 41, 83–106, 2003

STUDY ON BANDWIDTH OF 2-D DIELECTRIC PBG MATERIAL

L. G. Zheng and W. X. Zhang

State Key Laboratory of Millimeter Waves
Southeast University
Nanjing, Jiangsu, 210096, China

Abstract—Based on the eigenvalue equations of vector fields $\vec{E}$ and $\vec{H}$ by extending Bloch theorem to the vector field Maxwell equations, the characteristics of 2-D dielectric rod array with square cross-section elements arranged in square lattice is analyzed in detail. From the numerical results, empirical expressions for both the relative bandwidth of frequency band gap and the midgap frequency with respect to the average permittivity, under the optimal filling fraction of dielectric/air in cross-section for wider bandwidth, are formulated by means of data fit.

1. INTRODUCTION

The photonic band gap material consisting of dielectric structures with a periodic index of refraction has been investigated for more than a decade, in which the propagation of electromagnetic waves is forbidden. This kind of structure has been used to suppress spontaneous emission or to form a special waveguide, whose frequency range is located in the band gap.

After E. Yablonovitch and S. John reported their pioneer research in experiments [1–3], many others published their theoretical analyses, concerned with 3-D structures [4–9] or 2-D ones [10–23]. In classical analysis of a dielectric periodic structure, the eigenvalue equations are formulated by means of the plane wave expansion method of scalar field [5, 12] or vector field [4, 6–11, 13–23]. In numerical analysis, FDTD method is the first choice to carry out the wide-band frequency response of the periodic structure [24]. Transfer-matrix method is said to be a hybrid of time and frequency domain method, by which transmission spectrum can be retrieved directly [25, 26]. On the other hand, the task of engineers is to design the geometric parameters of the structure to satisfy a desired frequency response, rather than calculating the response from a given structure. In this article the simple formulation for relative bandwidth of frequency band-gap and the midgap frequency are provided, it must be a powerful tool in designing the PBG devices.

2. EIGENVALUE EQUATIONS FOR $\vec{E}$ AND $\vec{H}$

The study of waves in periodic structures makes use of a single physical principle proposed by Floquet in 1884. Later extension of the theorem by Bloch covers multidimensional periodic structures in his treatment of electrons in a crystal and is referred to as the Bloch expansion. It describes the characteristics of the state function satisfying scalar Schrödinger equation for an electron in a periodic potential formed by the atom lattice. Bloch Theorem states that [31]: The eigenstate ψ of the one-electron Hamiltonian $H = -\hbar^2\nabla^2/2m + U(\vec{r})$, where $U\left(\vec{r}+\vec{R}\right) = U(\vec{r})$ for all $\vec{R}$ in a Bravais lattice, can be chosen to have the form of a plane wave times a function with the periodicity of the Bravais lattice

$$\psi_{n\vec{k}}(\vec{r}) = e^{j\vec{k}\cdot\vec{r}}u_{n\vec{k}}(\vec{r}) = e^{j\vec{k}\cdot\vec{r}}u_{n\vec{k}}\left(\vec{r}+\vec{R}\right) \tag{1}$$

For the Maxwell's equations of vector fields $\vec{E}$ and $\vec{H}$, the plane wave expansion method was also employed in several references [3–22]. However, a rigorous derivation of Bloch theorem for vector fields satisfying Maxwell's equations had not been found yet to the authors' knowledge. The authors think that the derivation is necessary since there are so many differences between Schrödinger equation and Maxwell's equations. After an extensive study, it turns out that anyone can finish this work as long as he follows the steps presented in Solid State Physics [31] and it is too straightforward to be listed here. From now on, we'll directly employ Bloch Theorem on $\vec{E}$, $\vec{H}$, $\vec{D}$ and $\vec{B}$ in a periodic structure.

Assuming that the non-magnetic dielectric material under consideration is lossless, linear, anisotropic and periodically inhomogeneous. The relative permittivity in Maxwell equations is a dyadic (simply the subscript "r" is omitted)

$$\overline{\overline{\epsilon}}(\vec{r}) = \overline{\overline{\epsilon}}\left(\vec{r}+\vec{R}\right) \tag{2}$$

where $\vec{R}$ is Bravais lattice vector.

2.1. Eigenvalue Equation for Vector Field $\vec{E}$

The electric field $\vec{E}$ satisfies the following vector wave equation:

$$\nabla\times\nabla\times\vec{E}(\vec{r}) - \frac{\omega^2}{c^2}\overline{\overline{\epsilon}}(\vec{r})\cdot\vec{E}(\vec{r}) = \vec{0} \tag{3}$$

where ω is angular frequency, c is the velocity of light in free space. $\vec{E}(\vec{r})$ can be expressed in Bloch waves:

$$\vec{E}(\vec{r}) = \sum_{\vec{G}} \vec{E}_{\vec{G}} e^{j(\vec{k}+\vec{G})\cdot\vec{r}} \tag{4}$$

where $\vec{G}$ are reciprocal lattice vectors and $\vec{k}$ locates in the irreducible zone of the first Brillouin zone in reciprocal lattice space. $\overline{\overline{\epsilon}}(\vec{r})$ can be expressed in Fourier series as

$$\overline{\overline{\epsilon}}(\vec{r}) = \sum_{\vec{G}} \overline{\overline{\epsilon}}_{\vec{G}} e^{j\vec{G}\cdot\vec{r}} \tag{5}$$

where

$$\overline{\overline{\epsilon}}_{\vec{G}} = \frac{1}{V} \int_{\text{WS Cell}} \overline{\overline{\epsilon}}(\vec{r})\ e^{-j\vec{G}\cdot\vec{r}}\, dV \tag{6}$$

whose integral region is a Wigner-Seit cell (simply, WS Cell) with volume V. Substituting Eq. (4) and Eq. (5) into Eq. (3), the eigenvalue equation for electric field $\vec{E}$ has a form:

$$\left(\vec{k}+\vec{G}\right)\times\left(\vec{k}+\vec{G}\right)\times\vec{E}_{\vec{k}+\vec{G}} + \frac{\omega^2}{c^2}\sum_{\vec{G}'} \overline{\overline{\epsilon}}_{\vec{G}-\vec{G}'}\cdot\vec{E}_{\vec{k}+\vec{G}'} = \vec{0},\ \text{for each } \vec{G} \tag{7}$$

2.2. Eigenvalue Equation for Vector Field $\vec{H}$

The magnetic field $\vec{H}(\vec{r})$ satisfies the following wave equation:

$$\nabla\times\left[\overline{\overline{\eta}}(\vec{r})\cdot\left(\nabla\times\vec{H}(\vec{r})\right)\right] = \frac{\omega^2}{c^2}\vec{H}(\vec{r}) \tag{8}$$

where $\overline{\overline{\eta}}(\vec{r}) = \overline{\overline{\epsilon}}(\vec{r})^{-1}$ is also a dyadic with the same periodicity as $\overline{\overline{\epsilon}}(\vec{r})$.

By expanding $\vec{H}(\vec{r})$ in terms of Bloch waves as

$$\vec{H}(\vec{r}) = \sum_{\vec{G}} \vec{H}_{\vec{G}} e^{j(\vec{k}+\vec{G})\cdot\vec{r}} \tag{9}$$

and using the Fourier expansion for $\overline{\overline{\eta}}(\vec{r})$,

$$\overline{\overline{\eta}}(\vec{r}) = \sum_{\vec{G}} \overline{\overline{\eta}}_{\vec{G}} e^{j\vec{G}\cdot\vec{r}} \tag{10}$$

with its expansion coefficients

$$\overline{\overline{\eta}}_{\vec{G}} = \frac{1}{V} \int_{\text{WS Cell}} \overline{\overline{\eta}}(\vec{r})\ e^{-j\vec{G}\cdot\vec{r}}\, dV \tag{11}$$

one can get the following eigenvalue equation in reciprocal lattice space for vector field $\vec{H}(\vec{r})$:

$$\left(\vec{k}+\vec{G}\right)\times\sum_{\vec{G}'}\overline{\overline{\eta}}_{\vec{G}-\vec{G}'}\cdot\left[\left(\vec{k}+\vec{G}'\right)\times\vec{H}_{\vec{k}+\vec{G}'}\right]+\frac{\omega^2}{c^2}\vec{H}_{\vec{k}+\vec{G}}=\vec{0},\ \text{for each } \vec{G} \tag{12}$$

3. MODELING FOR COMPUTATION

3.1. Eigenvalue Equations in Matrix Form

The eigenvalue equation (7) of $\vec{E}$ can be simplified as (see Appendix A):

$$\overline{\overline{A}}_{\vec{G}}\cdot\vec{E}_{\vec{k}+\vec{G}}=\frac{\omega^2}{c^2}\sum_{\vec{G}'}\overline{\overline{\epsilon}}_{\vec{G}-\vec{G}'}\cdot\vec{E}_{\vec{k}+\vec{G}'},\ \text{for each } \vec{G} \tag{13}$$

where $\overline{\overline{A}}_{\vec{G}}=\left|\vec{k}+\vec{G}\right|^2\overline{\overline{I}}-\left(\vec{k}+\vec{G}\right)\left(\vec{k}+\vec{G}\right)$, $\overline{\overline{I}}$ is an identity dyadic.

Denoting

$$A=\begin{bmatrix}\overline{\overline{A}}_{\vec{G}_1} & \overline{\overline{0}} & \cdots & \overline{\overline{0}}\\ \overline{\overline{0}} & \overline{\overline{A}}_{\vec{G}_2} & \cdots & \overline{\overline{0}}\\ \vdots & \vdots & \ddots & \vdots\\ \overline{\overline{0}} & \overline{\overline{0}} & \cdots & \overline{\overline{A}}_{\vec{G}_N}\end{bmatrix}$$

$$B=\begin{bmatrix}\overline{\overline{\epsilon}}_{\vec{G}_1-\vec{G}_1} & \overline{\overline{\epsilon}}_{\vec{G}_1-\vec{G}_2} & \cdots & \overline{\overline{\epsilon}}_{\vec{G}_1-\vec{G}_N}\\ \overline{\overline{\epsilon}}_{\vec{G}_2-\vec{G}_1} & \overline{\overline{\epsilon}}_{\vec{G}_2-\vec{G}_2} & \cdots & \overline{\overline{\epsilon}}_{\vec{G}_2-\vec{G}_N}\\ \vdots & \vdots & \ddots & \vdots\\ \overline{\overline{\epsilon}}_{\vec{G}_N-\vec{G}_1} & \overline{\overline{\epsilon}}_{\vec{G}_N-\vec{G}_2} & \cdots & \overline{\overline{\epsilon}}_{\vec{G}_N-\vec{G}_N}\end{bmatrix}$$

$$X=\begin{bmatrix}\vec{E}_{\vec{k}+\vec{G}_1} & \vec{E}_{\vec{k}+\vec{G}_2} & \vec{E}_{\vec{k}+\vec{G}_3} & \cdots & \vec{E}_{\vec{k}+\vec{G}_N}\end{bmatrix}^T$$

where superscript "T" means transpose, N is the truncated number of reciprocal lattice points involved (i.e., the truncated number of the Fourier expansion terms), and $\overline{\overline{0}}$ is a zero dyadic. Then Eq. (13) can be rewritten as:

$$A\cdot X=\frac{\omega^2}{c^2}B\cdot X \tag{14}$$

where "$\cdot$" represents the dot-product operation between the elements of two matrices. This is the matrix form of the $\vec{E}$ eigenvalue equation, or say a generalized eigenvalue matrix equation.

The eigenvalue equation (12) of $\vec{H}$ can be rewritten as (see Appendix B):

$$\sum_{\vec{G}'} \overline{\overline{Y}}_{\vec{G}-\vec{G}'} \cdot \vec{H}_{\vec{k}+\vec{G}'} = -\frac{\omega^2}{c^2} \vec{H}_{\vec{k}+\vec{G}} \quad \text{for each } \vec{G} \tag{15}$$

where $\overline{\overline{Y}}_{\vec{G}-\vec{G}'} = \left(\vec{k}+\vec{G}\right) \times \overline{\overline{\eta}}_{\vec{G}-\vec{G}'} \times \left(\vec{k}+\vec{G}'\right)$.

Denoting

$$Z = \begin{bmatrix} \vec{H}_{\vec{k}+\vec{G}_1} & \vec{H}_{\vec{k}+\vec{G}_2} & \cdots & \vec{H}_{\vec{k}+\vec{G}_N} \end{bmatrix}^T,$$

$$Y = \begin{bmatrix} \overline{\overline{Y}}_{\vec{G}_1-\vec{G}_1} & \overline{\overline{Y}}_{\vec{G}_1-\vec{G}_2} & \cdots & \overline{\overline{Y}}_{\vec{G}_1-\vec{G}_N} \\ \overline{\overline{Y}}_{\vec{G}_2-\vec{G}_1} & \overline{\overline{Y}}_{\vec{G}_2-\vec{G}_2} & \cdots & \overline{\overline{Y}}_{\vec{G}_2-\vec{G}_N} \\ \vdots & \vdots & \ddots & \vdots \\ \overline{\overline{Y}}_{\vec{G}_N-\vec{G}_1} & \overline{\overline{Y}}_{\vec{G}_N-\vec{G}_2} & \cdots & \overline{\overline{Y}}_{\vec{G}_N-\vec{G}_N} \end{bmatrix},$$

then Eq. (15) has the form:

$$Y \cdot Z = -\frac{\omega^2}{c^2} Z \tag{16}$$

This is the matrix form of the $\vec{H}$ eigenvalue equation, i.e., an eigenvalue matrix equation.

By solving the above eigenvalue Eq. (14) or (16), the dispersive relation $\vec{k}$-ω may be abstracted.

3.2. Reciprocal Lattice Vector $\vec{G}$

In order to calculate the reciprocal lattice vector $\vec{G}$ in Eqs. (14) and (16), expanding it in terms of three basis vectors $\vec{b}_1$, $\vec{b}_2$, $\vec{b}_3$ as $\vec{G} = m\vec{b}_1 + n\vec{b}_2 + l\vec{b}_3$ (where m, n, l are independent integers), and employing these bases as

$$\vec{b}_1 = 2\pi \frac{\vec{a}_2 \times \vec{a}_3}{\vec{a}_1 \cdot (\vec{a}_2 \times \vec{a}_3)}, \quad \vec{b}_2 = 2\pi \frac{\vec{a}_3 \times \vec{a}_1}{\vec{a}_1 \cdot (\vec{a}_2 \times \vec{a}_3)}, \quad \vec{b}_3 = 2\pi \frac{\vec{a}_1 \times \vec{a}_2}{\vec{a}_1 \cdot (\vec{a}_2 \times \vec{a}_3)} \tag{17}$$

where $\vec{a}_1$, $\vec{a}_2$, $\vec{a}_3$ are the basis vectors of the direct geometric lattice [31].

In 2-D $\vec{k}$ space the basis vectors $\vec{b}_1$ and $\vec{b}_2$ can be expressed in form of $\vec{a}_1$ and $\vec{a}_2$ as

$$\vec{b}_1 = \frac{2\pi}{A} \vec{a}_2 \times \hat{z}$$

$$\vec{b}_2 = \frac{2\pi}{A}\hat{z} \times \vec{a}_1 \tag{18}$$

where A is the area of a WS Cell and $\hat{z}$ is the unit vector parallel to the axis of the rods.

3.3. The Fourier Coefficients of $\overline{\overline{\epsilon}}(\vec{r})$ and $\overline{\overline{\eta}}(\vec{r})$

Furthermore, the integrals of the Fourier coefficients $\overline{\overline{\epsilon}}_{\vec{G}}$ of $\overline{\overline{\epsilon}}(\vec{r})$ in expansion (6), and $\overline{\overline{\eta}}_{\vec{G}}$ of $\overline{\overline{\eta}}(\vec{r})$ in (11) must be estimated for Eqs. (14) and (16), respectively. Let $\overline{\overline{\xi}}(\vec{r})$ represents $\overline{\overline{\epsilon}}(\vec{r})$ or $\overline{\overline{\eta}}(\vec{r})$, and using subscripts "$a$" and "$b$" represent the inclusion and the host materials of the PBG structure, respectively, then the dyadic $\overline{\overline{\xi}}(\vec{r})$ can be expressed for any field point $\vec{r}$ and each lattice vector $\vec{R}$ as:

$$\overline{\overline{\xi}}(\vec{r}) = \overline{\overline{\xi}}_b + \left(\overline{\overline{\xi}}_a - \overline{\overline{\xi}}_b\right) \sum_{\vec{R}} u\left(\vec{r} - \vec{R}\right) \tag{19}$$

where the 3-D step-function

$$u\left(\vec{r} - \vec{R}\right) = \begin{cases} 0, & \text{when } \left(\vec{r} - \vec{R}\right) \text{ lies in the host material} \\ 1, & \text{when } \left(\vec{r} - \vec{R}\right) \text{ lies in the inclusion material} \end{cases}$$

Hence expressions (6) or Eq. (11) becomes

$$\begin{aligned} \overline{\overline{\xi}}_{\vec{G}} &= \frac{1}{V}\int_{\text{WS Cell}} \overline{\overline{\xi}}(\vec{r}) e^{-j\vec{G}\cdot\vec{r}}\, dV \\ &= \frac{1}{V}\int_{\text{WS Cell}} \left[\overline{\overline{\xi}}_b + \left(\overline{\overline{\xi}}_a - \overline{\overline{\xi}}_b\right) \sum_{\vec{R}} u\left(\vec{r} - \vec{R}\right)\right] e^{-j\vec{G}\cdot\vec{r}}\, dV \\ &= \begin{cases} \overline{\overline{\xi}}_b + \beta\left(\overline{\overline{\xi}}_a - \overline{\overline{\xi}}_b\right), & \text{when } \vec{G} = \vec{0} \\ \dfrac{1}{V}\left(\overline{\overline{\xi}}_a - \overline{\overline{\xi}}_b\right)\displaystyle\int_{\text{inclusion}} e^{-j\vec{G}\cdot\vec{r}}\, dV, & \text{when } \vec{G} \neq \vec{0} \end{cases} \end{aligned} \tag{20}$$

where $\beta = V_a/V$ is defined as "filling fraction", V_a is the volume of inclusion in a WS cell and the integral on WS cell is zero for $\vec{G} \neq \vec{0}$. In the case of isotropic material as $\overline{\overline{\epsilon}}_i = \epsilon_i \overline{\overline{I}}$ (where $i = a$ or b) for $\vec{E}$-equation; or $\overline{\overline{\eta}}_i = \epsilon_i^{-1} \overline{\overline{I}}$ (where $i = a$ or b) for $\vec{H}$-equation, $\overline{\overline{\xi}}$ can be degenerated appropriately and the characteristics of the PBG structure with respect to dyadic permittivity will be associated with the scalar dielectric constants ϵ_a and ϵ_b.

3.4. Notes about $\vec{E}$ and $\vec{H}$ Equations

Strictly speaking, only one matrix equation, Eq. (14) for electric field $\vec{E}$ or Eq. (16) for magnetic field $\vec{H}$ is necessary for the problem, the size of the matrix is changeable in different cases. Generally, the plane wave may be decomposited into TM and TE wave with respect to a specific vector. For 2-D rod structure, TM and TE wave are with respect to the axis of the rod. When Eq. (14) is employed, the matrix size will be $3N \times 3N$ due to three components of $\vec{E}$ in 3-D case, or $2N \times 2N$ due to two components of $\vec{E}$ in 2-D case with TE wave propagation, or $N \times N$ due to one component of $\vec{E}$ in 2-D case with TM wave propagation. On the other hand, when Eq. (16) is employed, the matrix size will also be $N \times N$ due to one component of $\vec{H}$ in 2-D case with TE wave. The benefit from employing both $\vec{E}$ and $\vec{H}$ equations is that fields for TM and TE waves can be calculated independently from the matrix equation with same size of $N \times N$. This will significantly reduce the computing time.

4. DISPERSION OF 2-D PBG STRUCTURE

In Eq. (14) or (16), vector $\vec{k}$ behaves as a parameter. For a given $\vec{k}$, a set of eigen frequencies can be obtained after solving this eigenvalue matrix equation. When $\vec{k}$ changes smoothly in one way or another, the eigen frequencies obtained will also change smoothly. For a homogeneous dielectric medium, all the frequencies should merge into one continuous band. For a PBG structure, however, due to its periodical inhomogeneity, the frequencies are grouped into separated bands. When the gap between two frequency bands appears for all the $\vec{k}$ within the first Brillouin zone and all the polarizations of the vector field ($\vec{E}$ or $\vec{H}$), it is called an absolute (complete) band gap. Absolute band gaps are more likely present in 3-D periodic structure [3–9]. In 2-D case, the larger band gaps with respect to a single polarization (TE or TM) are present for all the $\vec{k}$ within the first Brillouin zone, but they do not overlap each other. Researches intend to realize the overlap of the band gaps of different polarizations [18–20], and to find their engineering applications [21–23]. In this article, a 2-D structure with square lattice of square rods is fully analyzed.

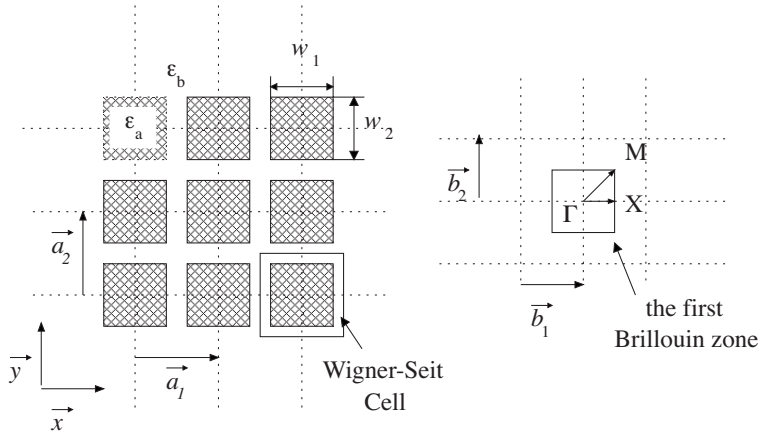

Figure 1. PBG structure with rectangular lattice of rectangular rods (a) in direct lattice ($\vec{r}$-) space; (b) in reciprocal lattice ($\vec{k}$-) space.

4.1. PBG Structure with Rectangular Lattice of Rectangular Rods

Fig. 1(a) shows the cross section of 2-D rectangular dielectric rods ($W_1 \times W_2$ in size) arranged in a rectangular lattice (basis vectors are $\vec{a}_1$ and $\vec{a}_2$). The relative permittivities of rod and background are ϵ_a and ϵ_b, respectively. The Wigner-Seit Cell is also shown. Fig. 1(b) shows the correspondent reciprocal lattice (its basis vectors are $\vec{b}_1$ and $\vec{b}_2$) and the first Brillouin zone. In this zone, point Γ means $\vec{k} = \vec{0}$ corresponding to the low frequency limit, point X means $\vec{k} = 0.5\vec{b}_1$, point M means $\vec{k} = 0.5\vec{b}_1 + 0.5\vec{b}_2$. The vector $\vec{k}$ changes magnitude but keeps its direction in $\vec{b}_1$ along segment $\overline{\Gamma X}$, changes both magnitude and direction from vector $\overline{\Gamma X}$ to $\overline{\Gamma M}$ along segment $\overline{XM}$, and changes magnitude but keeps its direction in $(\vec{b}_1 + \vec{b}_2)$ along segment $\overline{\Gamma M}$. Thus the $\vec{k}$-ω relation within the triangular area ($\triangle\overline{\Gamma XM}$) indicates the complete dispersion characteristics of the structure, due to the geometric symmetry of the first Brillouin zone.

Define refraction index ratio α as:

$$\alpha = \epsilon_> / \epsilon_< \tag{21}$$

where $\epsilon_> = \max(\epsilon_a, \epsilon_b)$, and $\epsilon_< = \min(\epsilon_a, \epsilon_b)$ for future use.

For rods of rectangular cross section arranged in rectangular

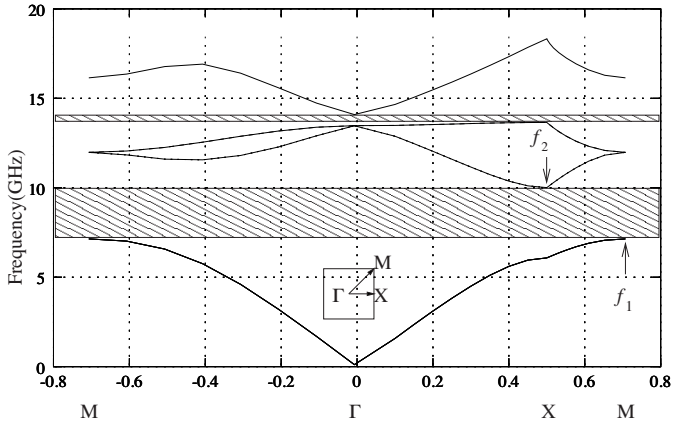

Figure 2. $\vec{k}$-ω curves for square rods ($W = 0.0048\,\mathrm{m}$, $\epsilon_a = 10.2$) arranged in square lattice in the air ($a = 0.012\,\mathrm{m}$, $\epsilon_b = 1.0$, $N = 11 \times 11$) from $\vec{E}$ equation with TM wave. The inset shows the first Brillouin zone.

lattice, the Fourier coefficients in Eq. (20) can be further evolved as:

$$\overline{\overline{\xi}}_{\vec{G}} = \begin{cases} \overline{\overline{\xi}}_b + \beta\left(\overline{\overline{\xi}}_a - \overline{\overline{\xi}}_b\right), & \text{when } \vec{G} = \vec{0} \\ \beta\left(\overline{\overline{\xi}}_a - \overline{\overline{\xi}}_b\right)[\sin(G_x W_1/2)/(G_x W_1/2)] & \\ \cdot\,[\sin(G_y W_2/2)/(G_y W_2/2)], & \text{when } \vec{G} \neq \vec{0} \end{cases} \tag{22}$$

where the filling fraction $\beta = W_1 W_2 / a_1 a_2$.

4.2. The $\vec{k}$-ω Relation

The PBG structure with square lattice of square rods is defined as $\vec{a}_1 = a\hat{x}$, $\vec{a}_2 = a\hat{y}$ and $W_1 = W_2 = W$. Let $N = N_1 \times N_2$, where N is the truncated number of the Fourier expansion terms or the truncated number of the reciprocal lattice points involved which can be divided into N_1 columns and N_2 rows.

The dispersion curves shown in Fig. 2 for the case of dielectric rods ($a = 0.012\,\mathrm{m}$, $W = 0.0048\,\mathrm{m}$, $\epsilon_b = 1.0$, $\epsilon_a = 10.2$ and $N = 121$) is calculated from the $\vec{E}$ equation (14) with TM wave, in which band gaps are outlined as the shadow strips. The lower and upper limits of the first gap are $f_1 = 7.1418\,\mathrm{GHz}$ and $f_2 = 10.009\,\mathrm{GHz}$, respectively. The dispersiveness with respect to the filling fraction β or refraction index ratio α will be focused at these two frequencies. Here the filling fraction is $\beta = 0.16$, the bandwidth of the gap for arbitrary propagation

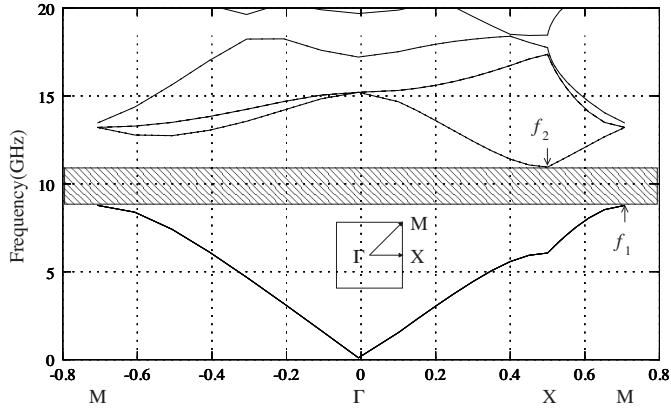

Figure 3. $\vec{k}$-ω curves for square air rods ($W = 0.01\,\mathrm{m}$, $\epsilon_a = 1.0$) arranged in square lattice in a host ($a = 0.012\,\mathrm{m}$, $\epsilon_b = 10.2$, $N = 29 \times 29$) from $\vec{H}$ equation with TE wave propagation. The inset shows the first Brillouin zone.

is $\Delta f = 2.8672\,\mathrm{GHz}$, the midgap Frequency is $f_0 = 8.5754\,\mathrm{GHz}$, and the relative bandwidth of the gap is $\Delta f/f_0 = 0.334$. The result shows good agreement with that in [23]. However, no gap was found for TE wave inside the same structure.

The dispersion curve shown in Fig. 3 for the case of air rods ($a = 0.012\,\mathrm{m}$, $W = 0.01\,\mathrm{m}$, $\epsilon_b = 10.2$, $\epsilon_a = 1.0$, $N = 841$) is calculated from the $\vec{H}$ equation (16) with TE wave, in which the first gap is outlined as shadow strip too. The lower and upper limits of this gap are $f_1 = 8.7754\,\mathrm{GHz}$ and $f_2 = 10.953\,\mathrm{GHz}$, respectively. Here the filling fraction $\beta = 0.694$, the bandwidth of this gap $\Delta f = 2.1776\,\mathrm{GHz}$, the midgap frequency $f_0 = 9.8642\,\mathrm{GHz}$, and the relative bandwidth $\Delta f/f_0 = 0.2207$. For TM wave propagation, there is only a very narrow band gap $\Delta f \approx 0.102\,\mathrm{GHz}$ exists inside the same structure.

4.3. Convergence Discussion

The plane wave expansion is a classical method for analysis of the characteristics of photonic crystal. It is also well known for its poor convergence, so the number of the expansion terms must be large enough in order to give out a reasonable result. In order to learn about the effect of the term number to the accuracy of the band gap, two cases are considered here: square lattice of square air rods/dielectric host and square lattice of square dielectric rods/air background, and different equations (14) and (16) are employed simultaneously for TE or TM

Table 1. Convergence calculations for square lattice ($a = 0.012\,\mathrm{m}$, $\epsilon_b = 1.0$) of square dielectric rods ($W = 0.0048\,\mathrm{m}$, $\epsilon_a = 10.2$) using TM wave $\vec{E}$ equation.

$N_1 \times N_2 = N$	11×11=121	15×15=225	21×21=441	29×29=841
f_1 (GHz)	7.1438	7.1429	7.1426	7.1424
f_2 (GHz)	10.009	10.007	10.005	10.005
$\Delta f = f_2 - f_1$ (GHz)	2.8672	2.8641	2.8624	2.8626
$f_0 = (f_2 + f_1)/2$ (GHz)	8.5754	8.5750	8.5738	8.5737
$\Delta f / f_0$	0.3344	0.3340	0.3339	0.3339

Table 2. Convergence calculations for square lattice ($a = 0.012\,\mathrm{m}$, $\epsilon_b = 1.0$) of square dielectric rods ($W = 0.0048\,\mathrm{m}$, $\epsilon_a = 10.2$) using TM wave $\vec{H}$ equation.

$N_1 \times N_2 = N$	11×11=121	15×15=225	21×21=441	29×29=841
f_1 (GHz)	7.5618	7.4535	7.3538	7.2967
f_2 (GHz)	10.739	10.531	10.381	10.276
$\Delta f = f_2 - f_1$ (GHz)	3.1772	3.0775	3.0272	2.9793
$f_0 = (f_2 + f_1)/2$ (GHz)	9.1504	8.9923	8.8674	8.7864
$\Delta f / f_0$	0.3472	0.3422	0.3414	0.3391

wave propagation respectively at different total cutoff N ($N = N_1 \times N_2$, N_1 and N_2 are cutoffs along the individual lattice base).

(1) TM wave in square lattice of square dielectric rods using $\vec{E}$ and $\vec{H}$ equations respectively

Table 1 presents the data calculated for the structure in Fig. 2: $a = 0.012\,\mathrm{m}$, $W = 0.0048\,\mathrm{m}$, $\epsilon_b = 1.0$, $\epsilon_a = 10.2$, by using $\vec{E}$ equation with TM wave. Frequencies f_1 and f_2 are also defined in Fig. 2.

Table 2 presents the data calculated for the same structure defined in Fig. 2 from $\vec{H}$ equation with the same TM wave.

The convergence trend of f_1 or f_2 in Table 2 is different from that in Table 1. It seems that for square lattice of dielectric rods, a reasonable result can be obtained in a relatively less terms of the expansion from solving $\vec{E}$ equation than from solving $\vec{H}$ equation with the same TM wave. The frequencies computed using MPB ([30]) for the same structure are: $f_1 = 7.1499\,\mathrm{GHz}$, $f_2 = 10.0157\,\mathrm{GHz}$,

Table 3. Convergence calculations for square lattice ($a = 0.012\,\mathrm{m}$, $\epsilon_b = 10.2$) of square air rods ($W = 0.01\,\mathrm{m}$, $\epsilon_a = 1.0$) from solving TE wave $\vec{E}$ equation.

$N_1 \times N_2 = N$	11×11=121	15×15=225	21×21=441	29×29=841
f_1 (GHz)	8.442	8.452	8.462	8.468
f_2 (GHz)	10.443	10.583	10.629	10.692
$\Delta f = f_2 - f_1$ (GHz)	2.001	2.131	2.167	2.224
$f_0 = (f_2 + f_1)/2$ (GHz)	9.443	9.518	9.546	9.58
$\Delta f / f_0$	0.222	0.224	0.227	0.232

Table 4. Convergence calculations for square lattice ($a = 0.012\,\mathrm{m}$, $\epsilon_b = 10.2$) of square air rods ($W = 0.01\,\mathrm{m}$, $\epsilon_a = 1.0$) from solving $\vec{H}$ equation with TE wave.

$N_1 \times N_2 = N$	11×11=121	15×15=225	21×21=441	29×29=841
f_1 (GHz)	9.486	9.038	8.958	8.775
f_2 (GHz)	11.205	11.087	10.991	10.953
$\Delta f = f_2 - f_1$ (GHz)	1.719	2.049	2.033	2.178
$f_0 = (f_2 + f_1)/2$ (GHz)	10.346	10.063	9.975	9.864
$\Delta f / f_0$	0.166	0.204	0.204	0.221

$f_0 = 8.5828\,\mathrm{GHz}$, $\Delta f/f_0 = 0.333893$. A difference of 2% for $\Delta f/f_0$ using $\vec{H}$ equation ($N_1 \times N_2 = 441$) will be introduced, compared to the MPB result.

(2) TE wave in square lattice of air rods using $\vec{E}$ and $\vec{H}$ equations respectively

Table 3 presents the data calculated for the structure defined in Fig. 3: $a = 0.012\,\mathrm{m}$, $W = 0.01\,\mathrm{m}$, $\epsilon_b = 10.2$, $\epsilon_a = 1.0$, by solving $\vec{E}$ equation with TE wave. Frequencies f_1 and f_2 were defined in Fig. 3.

Table 4 presents the data calculated for the same structure defined in Fig. 3 by solving $\vec{H}$ equation with TE wave. Frequency f_1 or f_2 increases in Table 3 and decreases in Table 4 when N increases. This is due to the fact that, in $\vec{E}$ equation (14), the expansion term and the eigenvalue term happen to be on the same side and in $\vec{H}$ equation (24), they are on the different side and the truncating effect of the expansion will affect the eigenvalues in an opposite way. When N is large enough,

they (f_1 in Table 3 and Table 4, for example) should converge to the true value. One can find that $\vec{E}$ equation is more attractive than $\vec{H}$ equation with both TM and TE wave. This is not strange because if we rebuild $\overline{\overline{\epsilon}}(\vec{r})$ using Eq. (5) as well as $\overline{\overline{\eta}}(\vec{r})$ using Eq. (10), we will find that the cutoff has less influence to $\overline{\overline{\epsilon}}(\vec{r})$ due to its large peak value (not small than 1.0) than to $\overline{\overline{\eta}}(\vec{r})$ due to its small valley value (not great than 1.0) [8]. The only way to improve the convergence is to employ terms in Eq. (5) and Eq. (10) as many as possible. This can only be done by using iterative eigenvalue solver where no explicit matrix storage is necessary [27–29]. The frequencies computed by using MPB for the same structure are: $f_1 = 8.4194\,\mathrm{GHz}$, $f_2 = 10.7212\,\mathrm{GHz}$, $\Delta f/f_0 = 0.2405$. A difference of -3.3% for $\Delta f/f_0$ using $\vec{E}$ equation ($N_1 \times N_2 = 841$) or -8.2% using $\vec{H}$ equation($N_1 \times N_2 = 841$) will be introduced, compared to the MPB result.

5. THE BANDWIDTH OF THE GAP AND THE MIDGAP FREQUENCY

As well known that the frequency band gap is caused by the periodic dielectric structure in certain state, there will not be any band gap if no periodicity (i.e., $\epsilon_a = \epsilon_b$) presents. Nevertheless, how to choose the refraction index ratio α and the filling fraction β to maximize the gap bandwidth as well as how to predict the mid-gap frequency are interesting topics for engineering application of PBG structure.

5.1. The Relative Bandwidth of a Gap

Firstly, a review of notation in [8] is presented. The space-averaged permittivity $\overline{\epsilon}$ of the structure had been proposed:

$$\overline{\epsilon} = \epsilon_b + (\epsilon_a - \epsilon_b)\beta \tag{23}$$

By rewriting $\epsilon(\vec{r})$ in the form of

$$\epsilon(\vec{r}) = \overline{\epsilon}\,[1 + \epsilon_\Delta(\vec{r})] \tag{24}$$

it is obvious that no variation of $\epsilon(\vec{r})$ ($\epsilon_\Delta(\vec{r}) = 0$) presents, no band gap will appear. Defining norm operation as

$$\|\epsilon(\vec{r})\|^2 = \frac{1}{V_{cell}} \int_{\mathrm{WS\ cell}} d\vec{r}\,|\epsilon(\vec{r})|^2$$

Table 5. Numerical results for the square lattice ($a = 0.012\,\mathrm{m}$) of square dielectric rods at different refraction index ratio using $\vec{E}$ equation with TM wave ($N = 21 \times 21$).

$\alpha = \epsilon_a/\epsilon_b$	3	4	5	6	7	8	9	10	11
β_{max} (calculated)	0.242	0.213	0.191	0.174	0.160	0.147	0.131	0.128	0.119
β_{opt} (according to Eq. (25))	0.250	0.200	0.167	0.143	0.125	0.122	0.100	0.091	0.083
$\Delta f/f_0\|_{max}$ (calculated)	-0.0035	0.0826	0.148	0.200	0.243	0.279	0.311	0.339	0.363
$\Delta f/f_0\|_{opt}$ (calculated)	-0.0036	0.0823	0.145	0.194	0.234	0.274	0.295	0.318	0.343
relative difference(%)	-2.8	0.36	2.0	3.0	3.8	1.8	5.3	6.4	5.7
β_{max} (fitted using (28))	0.248	0.211	0.186	0.168	0.155	0.145	0.137	0.130	0.124
$\Delta f/f_0\|_{max}$ (fitted using (29))	-0.022	0.088	0.162	0.214	0.254	0.284	0.309	0.329	0.345
$\Delta f/f_0\|_{opt}$ (fitted using (27)	0.000	0.100	0.167	0.214	0.250	0.278	0.300	0.318	0.333

The optimal value of filling fraction β_{opt} in the sense of maximizing the norm of $\epsilon_\Delta(\vec{r})$ was derived as

$$\beta_{opt} = \frac{\epsilon_b}{\epsilon_b + \epsilon_a} = \begin{cases} \dfrac{1}{1+\alpha}, & \alpha = \dfrac{\epsilon_a}{\epsilon_b} > 1 \\ \dfrac{\alpha}{1+\alpha}, & \alpha = \dfrac{\epsilon_b}{\epsilon_a} > 1 \end{cases} \tag{25}$$

and the space-averaged permittivity $\overline{\epsilon}$ became

$$\overline{\epsilon}|_{\beta_{opt}} = \frac{2\epsilon_b\epsilon_a}{\epsilon_b + \epsilon_a} = \begin{cases} \epsilon_b \dfrac{2\alpha}{1+\alpha}, & \alpha = \dfrac{\epsilon_a}{\epsilon_b} > 1 \\ \epsilon_a \dfrac{2\alpha}{1+\alpha}, & \alpha = \dfrac{\epsilon_b}{\epsilon_a} > 1 \end{cases} \tag{26}$$

for given ϵ_a and ϵ_b of materials [8].

Secondly, denoting $\Delta f/f_0|_{opt}$ as the relative gap bandwidth at β_{opt}, and $\Delta f/f_0|_{max}$ as the maximum relative gap bandwidth at β_{max} for given ϵ_a and ϵ_b. In order to find out the relationship among $\Delta f/f_0|_{max}$, $\Delta f/f_0|_{opt}$ and $\overline{\epsilon}|_{\beta_{opt}}$ as well as the relation between β_{opt} and β_{max}, extensive computation were made.

5.1.1. Square Lattice of Square Dielectric Rods

In the upper part of Table 5 the data were obtained by solving TM wave $\vec{E}$ equation at a set of values of the filling fraction β for given refraction index ratio α. The difference between $\Delta f/f_0|_{max}$ and $\Delta f/f_0|_{opt}$ is very small and one can use $\Delta f/f_0|_{opt}$ to predict $\Delta f/f_0|_{max}$ without significant accuracy loss. The most important discovery is that the curve of the normalized and shifted space-averaged

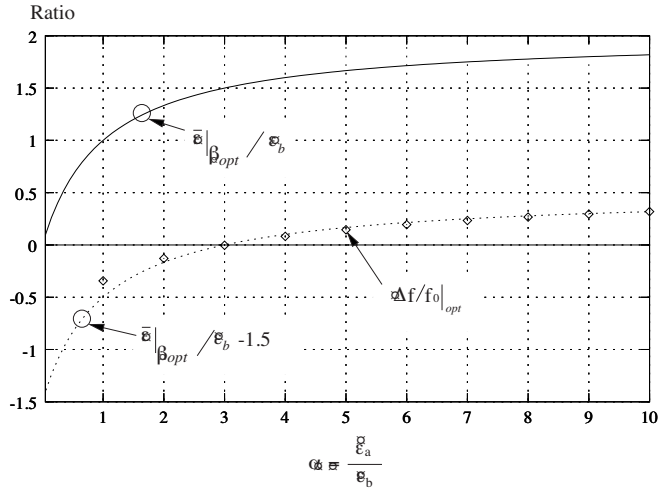

Figure 4. Relationship between the relative bandwidth of the first gap and the space-averaged permittivity for square dielectric rods arranged in square lattice in the air ($a = 0.012\,\mathrm{m}$, $\epsilon_b = 1.0$). The solid curve stands for $\overline{\epsilon}|_{\beta_{opt}}/\epsilon_b$. The dotted curve stands for $\overline{\epsilon}|_{\beta_{opt}}/\epsilon_b\Big|_{shifted}$. The diamond points stand for the calculated $\Delta f/f_0|_{opt}$ data at β_{opt}.

permittivity $\left.\frac{\overline{\epsilon}|_{\beta_{opt}}}{\epsilon_b}\right|_{shifted}$ is nearly identical to that of $\Delta f/f_0|_{opt}$ (See Fig. 4) and can be written in the mathematic expression:

$$\left.\frac{\Delta f}{f_0}\right|_{opt} \cong \left.\frac{\overline{\epsilon}|_{\beta_{opt}}}{\epsilon_b}\right|_{shifted} = \frac{\overline{\epsilon}|_{\beta_{opt}}}{\epsilon_b} - 1.5 = \frac{2\alpha}{(1+\alpha)} - 1.5 \tag{27}$$

where $\alpha = \epsilon_a/\epsilon_b > 1$.

Using this expression, one can predict the relative bandwidth of the first gap for square lattice of square rods for given ϵ_a and ϵ_b directly.

Furthermore, from a least square fit of the data, one can obtain fitting formulae for β_{max} and $\Delta f/f_0|_{max}$:

$$\beta_{max} \cong 0.746\frac{1}{1+\alpha} + 0.0619 \tag{28}$$

$$\left.\frac{\Delta f}{f_0}\right|_{max} \cong 1.102\frac{2\alpha}{1+\alpha} - 1.675 \tag{29}$$

where $\alpha = \epsilon_a/\epsilon_b > 1$. These formulae are based on the expression of β_{opt} and $\overline{\epsilon}|_{\beta_{opt}}$, respectively. The data calculated from expressions

Table 6. Numerical results by solving TE wave $\vec{H}$ equation for square lattice ($a = 0.012\,\mathrm{m}$) of square air rods ($N = 21 \times 21$).

$\alpha = \epsilon_b/\epsilon_a$	5	6	7	8	9	10	11
β_{max} (calculated)	0.510	0.568	0.600	0.606	0.614	0.619	0.627
β_{opt} (from Exp. (25))	0.833	0.857	0.875	0.888	0.900	0.909	0.917
$\Delta f/f_0\|_{max}$(calculated)	0.018	0.070	0.118	0.160	0.197	0.230	0.261
β_{max} (fitted from Exp. (30))	0.531	0.562	0.585	0.603	0.618	0.630	0.640
$\Delta f/f_0\|_{max}$ (fitted from Exp. (31))	0.006	0.0754	0.128	0.168	0.200	0.227	0.249
difference between $4th$ and $6th$ row (%)	-	-7.43	-8.13	-4.88	-1.5	1.3	4.71

(27), (28) and (29) are also presented in the lower part of Table 5 for comparison purpose.

5.1.2. Square Lattice of Square Air Rods

For Square lattice of square air rods, α is defined as: $\alpha = \epsilon_b/\epsilon_a > 1$. In this case, the filling fraction β_{max} with respect to the maximum gap bandwidth $\Delta f/f_0|_{max}$ is not coincided with β_{opt}. To make things worse, at β_{opt} , there is no all direction band gap for every α. Data in Table 6 are obtained by solving TE wave $\vec{H}$ equation for square lattice ($a = 0.012\,\mathrm{m}$, $N = 21 \times 21 = 441$) of square air rods at a set of β values.

Again from a least square fit of the data, one can obtain the following fitting formulae:

$$\beta_{max} \cong 1.41\beta_{opt} - 0.65 = 1.41\frac{\alpha}{1+\alpha} - 0.65 \tag{30}$$

$$\left.\frac{\Delta f}{f_0}\right|_{max} \cong 1.46\frac{\overline{\epsilon}|_{\beta_{opt}}}{\epsilon_a} - 2.42 = 1.46\frac{2\alpha}{1+\alpha} - 2.42 \tag{31}$$

where $\alpha = \epsilon_b/\epsilon_a > 1$. The data calculated from expressions (30) and (31) are also presented in the second part of Table 6 for comparison.

With expressions pair (25) and (27) or (28) and (29) or (30) and (31), one can readily predict the maximum relative gap bandwidth for dielectric rods or air rods when refraction index ratio $\alpha > 1$ is given.

5.2. The Wavelength of the Midgap Frequency in Free Space

In the same way, we can obtain a fit formula for the wavelength of the midgap frequency in free space.

Table 7. Normalized wavelength of the midgap frequency in free space (calculated and fitted) when $\epsilon_b = 1.0$, $a = 0.006\,\mathrm{m}$ for square lattice of square dielectric rods.

ϵ_a	3	4	5	6	7	8	9	10	11
$\alpha = \frac{\epsilon_a}{\epsilon_b}$	3	4	5	6	7	8	9	10	11
$\lambda_0/a\|_{\beta_{opt}}$ (calculated)	2.194	2.296	2.363	2.409	2.444	2.471	2.492	2.510	2.524
$\lambda_0/a\|_{\beta_{opt}}$ (fitted)	2.200	2.300	2.367	2.414	2.450	2.478	2.500	2.518	2.533
relative difference (%)	0.6	0.17	0.17	0.2	0.24	0.28	0.32	0.32	0.36
$\lambda_0/a\|_{\beta_{max}}$ (calculated)	2.194	2.332	2.419	2.511	2.581	2.633	2.668	2.689	2.754
$\lambda_0/a\|_{\beta_{max}}$ (fitted)	2.161	2.333	2.448	2.530	2.592	2.640	2.678	2.709	2.736
relative difference (%)	1.5	0.0	-1.2	-0.8	-0.4	-0.3	-0.4	-0.7	0.7

5.2.1. Square Lattice of Square Dielectric Rods

For square lattice of square dielectric rods, the fit formula for the wavelength of the midgap frequency in free space at β_{opt} is:

$$\left.\frac{\lambda_0}{a}\right|_{\beta_{opt}} \cong \sqrt{\epsilon_b}\left(\frac{\overline{\epsilon}|_{\beta_{opt}}}{\epsilon_b} + 0.7\right) = \sqrt{\epsilon_b}\left(\frac{2\alpha}{\alpha+1} + 0.7\right) \tag{32}$$

where $\alpha = \frac{\epsilon_a}{\epsilon_b} > 1$ and the fit formula for the wavelength of the midgap frequency in free space at β_{max} is:

$$\left.\frac{\lambda_0}{a}\right|_{\beta_{max}} \cong \sqrt{\epsilon_b}\left(1.725\frac{\overline{\epsilon}|_{\beta_{opt}}}{\epsilon_b} - 0.427\right) = \sqrt{\epsilon_b}\left(1.725\frac{2\alpha}{\alpha+1} - 0.427\right) \tag{33}$$

Table 7 shows the difference between the calculated and fitted wavelength of the midgap frequency at β_{opt} and β_{max} when $\epsilon_b = 1.0$, $a = 0.006\,\mathrm{m}$.

Table 8 shows the difference between the calculated and fitted wavelength of the midgap frequency at β_{opt} and β_{max} when $\epsilon_b = 3.0$, $a = 0.036\,\mathrm{m}$.

5.2.2. Square Lattice of Square Air Rods

The fit formula for the wavelength of the midgap frequency in free space is:

$$\left.\frac{\lambda_0}{a}\right|_{\beta_{max}} \cong \sqrt{\epsilon_a}\left(1.73\frac{2\alpha}{\alpha+1} - 0.43\right) \tag{34}$$

where $\alpha = \frac{\epsilon_b}{\epsilon_a} > 1$.

Table 8. Normalized wavelength of the midgap frequency in free space (calculated and fitted) when $\epsilon_b = 3.0$, $a = 0.036$ m for square lattice of square dielectric rods.

ϵ_a	9	23	15	18	21	24	27	30	33
$\alpha = \epsilon_a/\epsilon_b$ ($\epsilon_{b=3.0}$)	3	4	5	6	7	8	9	10	11
$\lambda_0/a\|_{\beta_{opt}}$ (calculated)	3.801	3.977	4.092	4.173	4.233	4.280	4.317	4.347	4.372
$\lambda_0/a\|_{\beta_{opt}}$ (fitted)	3.811	3.984	4.099	4.182	4.244	4.292	4.330	4.362	4.388
relative difference (%)	0.26	0.18	0.17	0.21	0.26	0.28	0.3	0.34	0.36
$\lambda_0/a\|_{\beta_{max}}$ (calculated)	3.734	4.037	4.209	4.349	4.449	4.554	4.632	4.687	4.776
$\lambda_0/a\|_{\beta_{max}}$ (fitted)	3.743	4.041	4.240	4.382	4.489	4.573	4.638	4.692	4.739
relative difference (%)	-0.3	-0.1	-1.0	-1.1	-1.3	-0.6	-0.2	-0.2	1.1

Table 9. Normalized wavelength of the midgap frequency in free space (calculated and fitted) when $\epsilon_a = 1.0$, $a = 0.012$ m for square lattice of square air rods.

ϵ_b	5	6	7	8	9	10	11
$\alpha(\epsilon_a = 1.0)$	5	6	7	8	9	10	11
$\lambda_0/a\|_{\beta_{max}}$ (calculated)	2.47	2.52	2.54	2.59	2.67	2.70	2.77
$\lambda_0/a\|_{\beta_{max}}$ (fitted)	2.44	2.52	2.58	2.63	2.67	2.70	2.73
relative difference(%)	1.2	0.0	-1.6	-1.5	0.0	0.0	1.5

Table 10. Normalized wavelength of the midgap frequency in free space (calculated and fitted) when $\epsilon_a = 3.0$, $a = 0.036$ m for square lattice of square air rods.

ϵ_b	15	18	21	24	27	30	33
$\alpha(\epsilon_a = 3.0)$	5	6	7	8	9	10	11
$\lambda_0/a\|_{\beta_{max}}$ (calculated)	4.247	4.365	4.403	4.533	4.614	4.677	4.788
$\lambda_0/a\|_{\beta_{max}}$ (fitted)	4.249	4.392	4.499	4.582	4.649	4.703	4.749
relative difference(%)	-0.04	-0.61	-2.2	-1.1	-0.8	-0.6	0.8

Table 9 shows the difference between the calculated and fitted wavelength of the midgap frequency at β_{max} when $\epsilon_a = 1.0$, $a = 0.012$ m.

Table 10 shows the difference between the calculated and fitted wavelength of the midgap frequency at β_{max} when $\epsilon_a = 3.0$, $a = 0.036$ m.

5.3. New Concept in Designing 2-D Dielectric PBG Structure

By means of the fitting formulae (27)–(34) mentioned above, for 2-D PBG structure of square dielectric rods arranged in square lattice , it is not necessary to solve eigenvalue equation, or do complicated numerical computation for designing its structure parameters. A programmable calculator is powerful enough to finish the task in the following steps:

(1) To determine the index ratio $\alpha = \epsilon_>/\epsilon_<$ by using Eq. (27) or (29) or (31) for a desired (maximum) gap bandwidth $\Delta f/f_0$.

(2) To determine the lattice parameters a, ϵ_b and ϵ_a by using Eq. (32) or (34) for a desired midgap wavelength λ_0 in free space.

(3) To determine the cross section size of the rods W by using Eq. (25) or (28) or (30).

These procedures can be followed for other PBG structure as long as the relations similar to (27)–(34) are established.

6. CONCLUSION

Plane wave expansion is a powerful method to analyze dielectric PBG structure. By extending Bloch theorem to Electromagnetic wave case, not only do we establish a solid theoretical foundation, but also provide two general eigenvalue equations, which can be used to analyze linear, lossless, anisotropic, multi-dimensional, dielectric PBG structure. Numerical analysis of 2-D dielectric PBG material shows that simple relationships exist between the bandwidth of the gap or midgap frequency and the parameters of the structure (filling fraction, refraction index ratio, periodicity, space average permittivity, etc.). It is also found that the structure of the square lattice of square dielectric rods possesses larger maximum bandwidth of the first gap than that of the square lattice of square air rods at the same given refraction index ratio. Future work will be carried out on other geometry in 2-D structure (circular or other shape of the rod cross section, other lattice geometry) and also in 3-D structure.

APPENDIX A. THE SIMPLIFICATION OF TRI-VECTOR CROSS PRODUCT

$$\vec{w}\times\vec{w}\times\vec{E}=\begin{vmatrix} \widehat{x} & \widehat{y} & \widehat{z} \\ w_x & w_y & w_z \\ w_yE_z - w_zE_y & w_zE_x - w_xE_z & w_xE_y - w_yE_x \end{vmatrix}$$

$$
\begin{aligned}
& \widehat{x}\left(w_y w_x E_y - w_y^2 E_x - w_z^2 E_x + w_x w_z E_z\right) \\
= & -\widehat{y}\left(w_x^2 E_y - w_x w_y E_x + w_z^2 E_y - w_y w_z E_z\right) \\
& +\widehat{z}\left(w_x w_z E_x - w_x^2 E_z - w_y^2 E_z + w_z w_y E_y\right) \\
& \widehat{x}[(-w_y^2 - w_z^2)\widehat{x} + w_y w_x \widehat{y} + w_x w_z \widehat{z}] \cdot (E_x \widehat{x} + E_y \widehat{y} + E_z \widehat{z}) \\
= & +\widehat{y}[w_x w_y \widehat{x} + (-w_x^2 - w_z^2)\widehat{y} + w_y w_z \widehat{z}] \cdot (E_x \widehat{x} + E_y \widehat{y} + E_z \widehat{z}) \\
& +\widehat{z}[w_x w_z \widehat{x} + w_z w_y \widehat{y} + (-w_x^2 - w_y^2)\widehat{z}] \cdot (E_x \widehat{x} + E_y \widehat{y} + E_z \widehat{z}) \\
= & \begin{bmatrix} -(w_x^2 + w_y^2 + w_z^2)(\widehat{x}\widehat{x} + \widehat{y}\widehat{y} + \widehat{z}\widehat{z}) \\ +w_x^2 \widehat{x}\widehat{x} + w_y w_x \widehat{x}\widehat{y} + w_x w_z \widehat{x}\widehat{z} \\ +w_x w_y \widehat{y}\widehat{x} + w_y^2 \widehat{y}\widehat{y} + w_y w_z \widehat{y}\widehat{z} \\ +w_x w_z \widehat{z}\widehat{x} + w_z w_y \widehat{z}\widehat{y} + w_z^2 \widehat{z}\widehat{z} \end{bmatrix} \cdot (E_x \widehat{x} + E_y \widehat{y} + E_z \widehat{z}) \\
= & \left(-|\vec{w}|^2 \overline{\overline{I}} + \vec{w}\vec{w}\right) \cdot \vec{E}
\end{aligned} \tag{A1}
$$

APPENDIX B. SIMPLIFICATION OF THE VECTOR-DYADIC EXPRESSION

By using dyadic identity:

$$
\begin{aligned}
\overline{\overline{A}} \cdot \left(\vec{a} \times \vec{b}\right) &= \left(\overline{\overline{A}} \times \vec{a}\right) \cdot \vec{b} \\
\vec{a} \times \left(\overline{\overline{A}} \cdot \vec{b}\right) &= \left(\vec{a} \times \overline{\overline{A}}\right) \cdot \vec{b}
\end{aligned}
$$

We have:

$$
\begin{aligned}
\vec{w} \times \left[\overline{\overline{\eta}} \cdot \left(\vec{w}' \times \vec{H}\right)\right] &= \vec{w} \times \left[(\overline{\overline{\eta}} \times \vec{w}') \cdot \vec{H}\right] \\
&= (\vec{w} \times \overline{\overline{\eta}} \times \vec{w}') \cdot \vec{H}
\end{aligned} \tag{B1}
$$

REFERENCES

1. Yablonovitch, E., "Inhibited spontaneous emission in solid-state physics and electronics," *Phys. Rev. Lett.*, Vol. 58, No. 2, 2059–2062, 1987.
2. John, S., "Strong localization of photons in certain disordered dielectric superlattice," *Phys. Rev. Lett.*, Vol. 58, 2486, 1987.
3. Yablonovitch, E. and T. J. Gmitter, "Photonic band structure: The face-centered-cubic case," *Phys. Rev. Lett.*, Vol. 63, 1950, 1989.
4. Leung, K. M. and Y. F. Liu, "Full vector wave calculation of photonic band structures in face-centered-cubic dielectric media," *Phys. Rev. Lett.*, Vol. 65, No. 21, 2646–2649, 1990.

5. Satpathy, S. and Z. Zhang, "Theory of photon bands in three-dimensional periodic dielectric structures," *Phys. Rev. Lett.*, Vol. 64, No. 11, 1239–1242, 1990.
6. Zhang, Z. and S. Satpathy, "Electromagnetic wave propagation in periodic structures: Bloch wave solution of Maxwell's equations," *Phys. Rev. Lett.*, Vol. 65, No. 21, 2650–2653, 1990.
7. Ho, K. M., C. T. Chan, and C. M. Soukoulis, "Existence of a photonic gap in periodic dielectric structures," *Phys. Rev. Lett.*, Vol. 65, No. 25, 3152–3155, 1990.
8. Sözüer, H. S. and J. W. Haus, "Photonic bands: Convergence problems with the plane-wave method," *Phys. Rev. B*, Vol. 45, No. 24, 13962–13972, June 15, 1992.
9. Kweon, G.-I. and N. M. Lawandy, "Quantum electrodynamics in photonic crystals," *Optics Communications*, Vol. 118, 388–411, 1995.
10. Plihal, M., A. Shambrook, A. A. Maradudin, and P. Sheng, "Two-dimensional photonic band structures," *Opt. Commun.*, Vol. 80, No. 3, 4, 199–204, 1991.
11. Plihal, M. and A. A. Maradudin, "Photonic band structure of two-dimensional systems: The triangular lattice," *Phys. Rev. B*, Vol. 44, No. 16, 8565–8571, 1991.
12. McCall, S. L., P. M. Platzman, R. Dalichaouch, D. Smith, and S. Schultz, "Microwave propagation in two-dimensional dielectric lattices," *Phys. Rev. Lett.*, Vol. 67, No. 15, 2017–2020, 1991.
13. Villeneuve, P. R. and M. Piché, "Photonic band gaps in two-dimensional square and hexagonal lattices," *Phys. Rev. B, Condens. Matter*, Vol. 46, No. 8, 4969–4972, Aug. 1992.
14. Villeneuve, P. R. and M. Piché, "Photonic band gaps in two-dimensional square lattices: Square and circular rods," *Phys. Rev. B, Condens. Matter*, Vol. 46, No. 8, 4973–4975, Aug. 1992.
15. Padjen, R., J. M. Gerard, and J. Y. Marzin, "Analysis of the filling pattern dependence of the photonic bandgap for two-dimensional systems," *Journal of Modern Optics*, Vol. 41, No. 2, 295–310, 1994.
16. Maradudin, A. A. and A. R. McGurn, "Out of plane propagation of electromagnetic waves in a two-dimensional periodic dielectric medium," *Journal of Modern Optics*, Vol. 41, No. 2, 275–284, 1994.
17. Villeneuve, P. R. and M. Piché, "Photonic band gaps of transverse-electric modes in two-dimensionally periodic media," *J. Opt. Soc. Am. A*, Vol. 8, No. 8, 1296–1305, 1991.
18. Anderson, C. M. and K. P. Giapis, "Larger two-dimensional

photonic band gaps," *Phys. Rev. Lett.*, Vol. 77, No. 14, 2949–2952, 1996.

19. Qiu, M. and S. He, "Large complete band gap in two-dimensional photonic crystals with elliptic air holes," *Phys. Rev. B*, Vol. 60, No. 15, 10610–10612, 1999.
20. Li, Z.-Y., B.-Y. Gu, and G.-Z. Yang, "Large absolute band gap in 2D anisotropic photonic crystals," *Phys. Rev. Lett.*, Vol. 81, No. 12, 2574–2577, 1998.
21. Yang, H.-Y. D., "Surface-wave elimination in integrated circuit structures with artificial periodic materials," *Electromagnetics*, Vol. 20, 125–130, 2000.
22. Gonzalo, R., P. de Maagt, and M. Sorolla, "Enhanced patch-antenna performance by suppressing surface waves using photonic-bandgap substrates," *IEEE Trans. on MTT*, Vol. 47, No. 11, 2131–2138, Nov. 1999.
23. Shumpert, J. D., W. J. Chappell, and L. P. B. Katehi, "Parallel-plate mode reduction in conductor-backed slots using electromagnetic bandgap substrates," *IEEE Trans. on MTT*, Vol. 47, No. 11, 2099–2104, Nov. 1999.
24. Fan, S., P. R. Villeneuve, and J. D. Joannopoulos, "Large omnidirectional band gaps in metallodielectric photonic crystals," *Phys. Rev. B, Condens. Matter*, Vol. 54, No. 16, 11245–11251, Oct. 1996.
25. Felbacq, D., G. Tayeb, and D. Maystre, "Scattering by a random set of parallel cylinders," *J. Opt. Soc. Am. A*, Vol. 11, No. 9, 2526–2538, Sept. 1994.
26. Bell, P. M., J. B. Pendry, L. M. Moreno, and A. J. Ward, "A program for calculating photonic band structures and transmission coefficients of complex structures," *Comput. Phys. Comm.*, Vol. 85, 306–322, 1995.
27. Meade, R. D., A. M. Rappe, K. D. Brommer, J. D. Joannopoulos, and O. L. Alerhand, "Accurate theoretical analysis of photonic band-gap materials," *Phys. Rev. B*, Vol. 48, 8434–8437, 1993. Erratum: S. G. Johnson, ibid, Vol. 55, 15942, 1997.
28. Johnson, S. G. and J. D. Joannopoulos, "Block-iterative frequency-domain methods for Maxwell's equations in a planewave basis," *Optics Express*, Vol. 8, No. 3, 173–190, 2001.
29. Joannopoulos, J. D., R. D. Meade, and J. N. Winn, *Photonic Crystals: Molding the Flow of Light*, Princeton, 1995.
30. Johnson, S. G. and J. D. Joannopoulos, *The MIT Photonic-Bands Package*, http://ab-initio.mit.edu/mpb/.

31. Ashcroft, N. W. and N. D. Mermin, *Solid State Physics*, Chapter 8, Holt-saunders International Editions, 1976.